

We are IntechOpen, the world's leading publisher of Open Access books Built by scientists, for scientists

6,900

Open access books available

186,000

International authors and editors

200M

Downloads

Our authors are among the

154

Countries delivered to

TOP 1%

most cited scientists

12.2%

Contributors from top 500 universities



WEB OF SCIENCE™

Selection of our books indexed in the Book Citation Index
in Web of Science™ Core Collection (BKCI)

Interested in publishing with us?
Contact book.department@intechopen.com

Numbers displayed above are based on latest data collected.
For more information visit www.intechopen.com



Crashworthiness Investigation and Optimization of Empty and Foam Filled Composite Crash Box

Dr. Hamidreza Zarei¹ and Prof. Dr.-Ing. Matthias Kröger²

¹*Aeronautical University, Tehran,*

²*Institute of Machine Elements, Design and Manufacturing,
University of Technology Freiberg,*

¹*Iran*

²*Germany*

1. Introduction

Metallic and composite columns are used in a broad range of automotive and aerospace applications and especially as crash absorber elements. In automotive application, crashworthy structures absorb impact energy in a controlled manner. Thereby, they bring the passenger compartment to rest without subjecting the occupant to high decelerations. Energy absorption in metallic crash absorbers normally takes place by progressive buckling and local bending collapse of columns wall. A distinctive feature of such a deformation mechanism is that the rate of energy dissipation is concentrated over relatively narrow zones, while the other part of the structure undergoes a rigid body motion. In comparison to metals, most composite columns crush in a brittle manner and they fail through a sequence of fracture mechanism involving fiber fracture, matrix crazing and cracking, fiber-matrix debonding, delamination and internal ply separation. The high strength to weight and stiffness to weight ratios of composite materials motivated the automobile industry to gradual replacement of the metallic structures by composite ones. The implementation of composite materials in the vehicles not only increases the energy absorption per unit of weight (Ramakrishna, 1997) but also reduces the noise and vibrations, in comparison with steel or aluminum structures (Shin et al., 2002). The crashworthiness of a crash box is expressed in terms of its energy absorption E and specific energy absorption SEA. The energy absorption performance of a composite crash box can be tailored by controlling various parameters like fiber type, matrix type, fiber architecture, specimen geometry, process condition, fiber volume fraction and impact velocity. A comprehensive review of the various research activities have been conducted by Jacob et al. (Jacob et al., 2002) to understand the effect of particular parameter on energy absorption capability of composite crash boxes.

The response of composite tubes under axial compression has been investigated by Hull (Hull, 1982). He tried to achieve optimum deceleration under crush conditions. He showed that the fiber arrangement appeared to have the greatest effect on the specific energy absorption. Farley (Farley, 1983 and 1991) conducted quasi-static compression and impact tests to investigate the energy absorption characteristics of the composite tubes. Through his

experimental work, he showed that the energy absorption capabilities of Thornel 300-fiberite and Kevlar-49-fiberite 934 composites are a function of crushing speed. He concluded that strain rate sensibility of these composite materials depends on the relationship between the mechanical response of the dominant crushing mechanism and the strain rate. Hamada and Ramakrishna (Hamada & Ramakrishna, 1997) also investigate the crush behavior of composite tubes under axial compression. Carbon polyether etherketone (PEEK) composite tubes were tested quasi-statically and dynamically showing progressive crushing initiated at a chamfered end. The quasi-statically tested tubes display higher specific energy absorption as a result of different crushing mechanisms attributed to different crushing speeds. Mamalis et al. (Mamalis et al., 1997 and 2005) investigated the crush behavior of square composite tubes subjected to static and dynamic axial compression. They reported that three different crush modes for the composite tubes are included, stable progressive collapse mode associated with large amounts of crush energy absorption, mid-length collapse mode characterized by brittle fracture and catastrophic failure that absorbed the lowest energy. The load-displacement curves for the static testing exhibited typical peaks and valleys with a narrow fluctuation amplitude, while the curves for the dynamically tested specimens were far more erratic. Later Mamalis et al. (Mamalis et al., 2006) investigated the crushing characteristics of thin walled carbon fiber reinforced plastic CFRP tubular components. They made a comparison between the quasi-static and dynamic energy absorption capability of square CFRP.

The high cost of the experimental test and also the development of new finite element codes make the design by means of numerical methods very attractive. Mamalis et al. (Mamalis et al., 2006) used the explicit finite element code LS-DYNA to simulate the crush response of square CFRP composite tubes. They used their experimental results to validate the simulations. Results of experimental investigations and finite element analysis of some composite structures of a Formula One racing car are presented by Bisagni et al. (Bisagni et al., 2005). Hoermann and Wacker (Hoermann & Wacker, 2005) used LS-DYNA explicit code to simulate modular composite thermoplastic crash boxes. El-Hage et al. (El-Hage et al., 2004) used finite element method to study the quasi-static axial crush behavior of aluminum/composite hybrid tubes. The hybrid tubes contain filament wound E glass-fiber reinforced epoxy over-wrap around an aluminum tube.

Although there is several published work to determine the crash characteristics of metallic and composite columns, only few attempts have been made to optimize those behaviors. Yamazaki and Han (Yamazaki & Han, 1998) used crashworthiness maximization techniques for tubular structures. Based on numerical analyzes, the crash responses of tubes were determined and a response surface approximation method RSM was applied to construct an approximative design sub-problems. The optimization technique was used to maximize the absorbed energy of cylindrical and square tubes subjected to impact crash load. For a given impact velocity and material, the dimensions of the tube such as thickness and radius were optimized under the constraints of tube mass as well as the allowable limit of the axial impact force. Zarei and Kroeger (Zarei & Kroeger, 2006) used Multi design objective MDO crashworthiness optimization method to optimize circular aluminum tubes. Here the MDO procedure was used to find the optimum aluminum tube that absorbs the most energy while has minimum weight.

This study deals with experimental and numerical crashworthiness investigations of square and hexagonal composite crash boxes. Drop weight impact tests are conducted on composite crash boxes and the finite element method is used to reveal more details about crash process. Thin shell elements are used to model the tube walls. The crash experiments

show that tubes crush in a progressive manner, i.e. the crushing starts from triggered end of the tubes, exhibit delamination between the layers. Two finite element models, namely single layer and multi layers, are developed.

In the single layer model, the delamination behavior could not be modeled and the predicted energy absorption is highly underestimated. Therefore, to properly consider the delamination between the composite layers, the tube walls are modeled as multi layer shells and an adequate contact algorithm is implemented to model the adhesion between them. Numerical results show that in comparison to the one layer method, the multi layer method yield more meaningful and accurate experimental results. Finally the multi design optimization MDO technique is implemented to identify optimum tube geometry that has maximum energy absorption and specific energy absorption characteristics.

The length, thickness (number of layers) and width of the tubes are optimized while the mean crash load is not allowed to exceed allowable limits. The D-optimal design of experiment and the response surface method are used to construct sub-problems in the sequentially optimization procedure. The optimum tube is determined that has maximum reachable energy absorption with minimum tube weight. Finally the optimum composite crash box is compared with the optimum aluminum crash box. Also the crash behaviour of foam filled composite crash boxes are investigated and compared with empty ones.

2. Experimental and numerical results

Axial impact tests were conducted on square and hexagonal composite crash boxes. The nominal wall thicknesses of the composite tubes are 2 mm, 2.4 mm and 2.7 mm. Square tubes with length of 150 mm and hexagonal tube with the length of 91 mm are used, see Figure 1. The specimens are made from woven glass-fiber in a polyamide matrix, approximately 50% volume fiber. Equal amount of fibers are in the two perpendicular main orientations. They are produced by Jacob Composite GmbH. Similar tubes are used in the bumper system of the BMW M3 E46 as well as E92 and E93 model as crash boxes.

A 45 degree trigger was created at the top end of the specimens. Generally injection moulding can be used to produce complex reinforced thermoplastics parts with low fiber length/fiber diameter aspect ratio. With increasing aspect ratio the crush performance increases but the flow ability of the material decreases. For this reason continuous reinforced thermoplastic have to be thermoformed. In this way and by using other post processing technologies like welding, complex composite parts with an excellent crush performance can be realized (Hoermann & Wacker, 2005). Here, the crash boxes are produced from thermoplastic plates by using thermoforming technique. The square specimens have overlap in one side and the overlaps have been glued by using a structural adhesive. The hexagonal crash boxes consist of two parts that are welded to each other.

The experimental tests have been conducted on the drop test rig, see Fig. 2, which is installed in the Institute of Dynamics and Vibrations at the Leibniz University of Hannover. This test rig has an impact mass which can be varied from 20 to 300 kg. The maximum drop height is 8 m and maximum impact speed is 12.5 m/s. The force and the displacement are recorded with a PC using an AD-converter. The force is measured using strain gauges and laser displacement sensors provide the axial deformation distance of the tubes. Here an impact mass of 92 kg was selected. The interest in this study is the mean crashing load P_m and the energy absorption E . The mean crash load is defined by

$$P_m = 1 / \delta \int_0^\delta P(\delta) d\delta \quad (1)$$

where $P(\delta)$ is the instantaneous crash load corresponding to the instantaneous crash displacement d . The area under the crash load–displacement curve gives the absorbed energy. The ratio of the absorbed energy to the crush mass of the structure is the specific energy absorption. High values indicate a lightweight absorber. Figure 1 shows the geometry of the specimens.

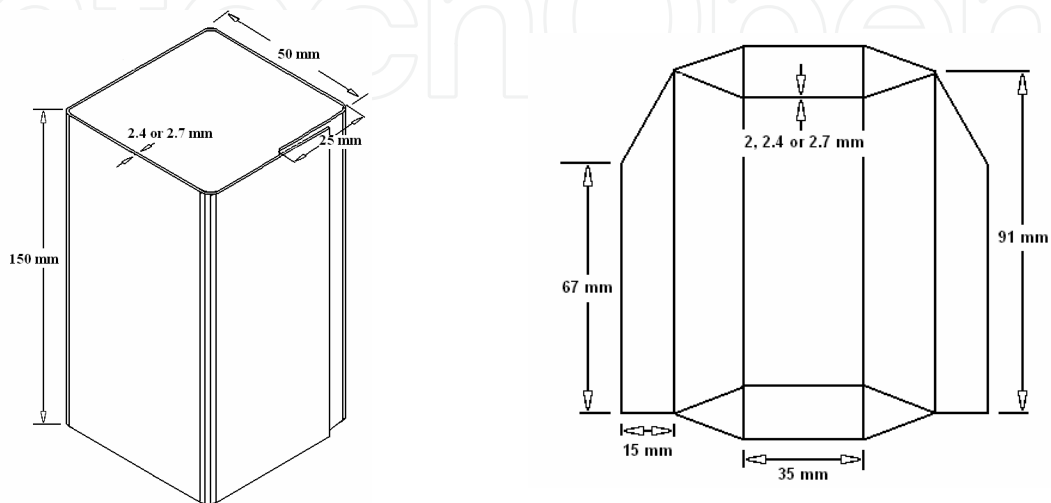


Fig. 1. (a) Square crash box (b) hexagonal crash box

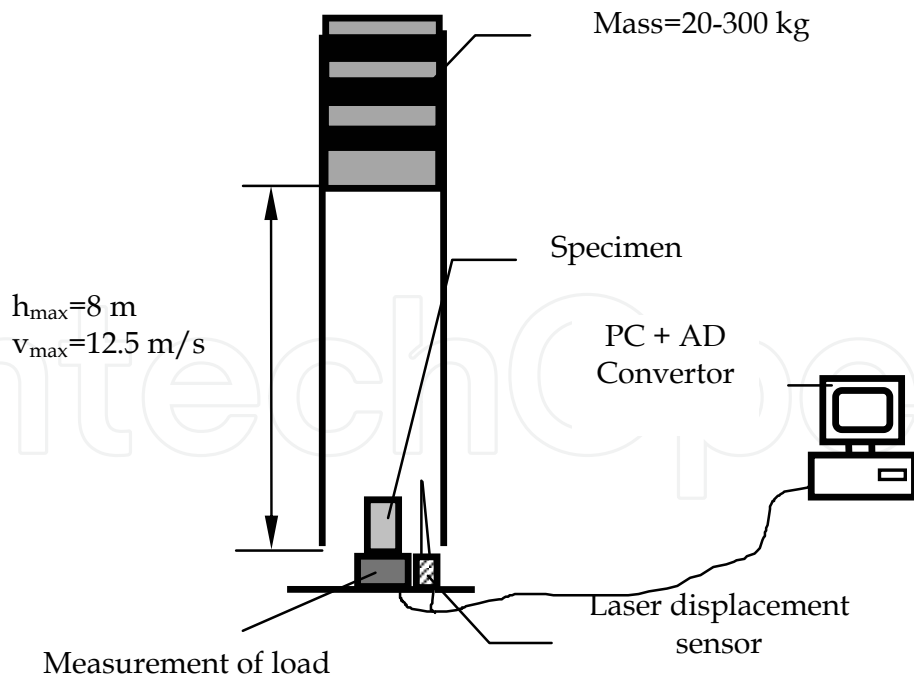


Fig. 2. Test rig

Numerical simulations of crash tests are performed to obtain local information from the crush process. The modeling and analysis is done with the use of explicit finite element

code, LS-DYNA. The column walls are built with the Belytschko-Tsay thin shell elements and solid elements are used to model the impactor. The contact between the rigid body and the specimen is modeled using a node to surface algorithm with a friction coefficient of $\mu=0.2$. To take into account the self contact between the tube walls during the deformation, a single surface contact algorithm is used. The impactor has been modeled with the rigid material. The composite walls have been modeled with the use of material model #54 in LS-DYNA. This model has the option of using either the Tsai-Wu failure criterion or the Chang-Chang failure criterion for lamina failure. The Tsai-Wu failure criterion is a quadratic stress-based global failure prediction equation and is relatively simple to use; however, it does not specifically consider the failure modes observed in composite materials (Mallick, 1990). Chang-Chang failure criterion (Mallick, 1990) is a modified version of the Hashin failure criterion (Hashin, 1980) in which the tensile fiber failure, compressive fiber failure, tensile matrix failure and compressive matrix failure are separately considered. Chang and Chang modified the Hashin equations to include the non-linear shear stress-strain behavior of a composite lamina. They also defined a post-failure degradation rule so that the behavior of the laminate can be analyzed after each successive lamina fails. According to this rule, if fiber breakage and/or matrix shear failure occurs in a lamina, both transverse modulus and minor Poisson’s ratio are reduced to zero, but the change in longitudinal modulus and shear modulus follows a Weibull distribution. On the other hand, if matrix tensile or compressive failure occurs first, the transverse modulus and minor Poisson’s ratio are reduced to zero, while the longitudinal modulus and shear modulus remain unchanged. The failure equations selected for this study are based on the Chang-Chang failure criterion. However, in material model #54, the post-failure conditions are slightly modified from the Chang-Chang conditions. For computational purposes, four indicator functions e_f , e_c , e_m , e_d corresponding to four failure modes are introduced. These failure indicators are based on total failure hypothesis for the laminas, where both the strength and the stiffness are set equal to zero after failure is encountered,

(a) Tensile fiber mode (fiber rupture),

$$\sigma_{aa} > 0, \text{ and } e_f^2 = (\sigma_{aa}/x_t)^2 + \zeta(\sigma_{ab}/S_c)^2 - 1 \begin{cases} \geq 0 \Rightarrow \text{faild} \\ > 0 \Rightarrow \text{elastic} \end{cases} \quad (2)$$

Where ζ is a weighting factor for the shear term in tensile fiber mode and $0 < \zeta < 1$. $E_a = E_b = G_{ab} = \nu_{ab} = \nu_{ba} = 0$ after lamina failure by fiber rupture.

(b) Compressive fiber mode (fiber buckling or kinking),

$$\sigma_{aa} > 0, \text{ and } e_c^2 = (\sigma_{aa}/x_c)^2 - 1 \begin{cases} \geq 0 \Rightarrow \text{faild} \\ > 0 \Rightarrow \text{elastic} \end{cases} \quad (3)$$

$E_a = \nu_{ab} = \nu_{ba} = 0$ after lamina failure by fiber buckling or kinking.

(c) Tensile matrix mode (matrix cracking under transverse tension and in-plane shear),

$$\sigma_{bb} > 0, \text{ and } e_m^2 = (\sigma_{bb}/y_t)^2 + \zeta(\sigma_{ab}/S_c)^2 - 1 \begin{cases} \geq 0 \Rightarrow \text{faild} \\ > 0 \Rightarrow \text{elastic} \end{cases} \quad (4)$$

$E_a=G_{ab}=v_{ab}=0$ after lamina failure by matrix cracking

(d) Compressive matrix mode (matrix cracking under transverse compression and in-plane shear),

$$\sigma_{bb} > 0, \text{ and } e_d^2 = (\sigma_{bb}/2S_c)^2 + [(y_c / 2S_c)^2 - 1] \sigma_{bb} / y_c + (\sigma_{bb}/2S_c)^2 - 1 \begin{cases} \geq 0 \Rightarrow \text{faild} \\ > 0 \Rightarrow \text{elastic} \end{cases} \quad (5)$$

$E_b= v_{ab}=v_{ba}=0 \rightarrow G_{ab}=0$ after lamina failure by matrix cracking

In Equations (2)–(5), σ_{aa} is the stress in the fiber direction, σ_{bb} is the stress in the transverse direction (normal to the fiber direction) and σ_{ab} is the shear stress in the lamina plane aa-bb. The other lamina-level notations in Equations (2)–(5) are as follows: x_t and x_c are tensile and compressive strengths in the fiber direction, respectively. Y_t and y_c are tensile and compressive strengths in the matrix direction, respectively. S_c is shear strength; E_a and E_b are Young's moduli in the longitudinal and transverse directions, respectively. Here, to model the trigger, two elements with progressively reduced thicknesses were placed in the triggers zone. The tied surface to surface contact algorithm has been used to glue the overlapping walls.

Tables 1 and 2 show the test results of the square and hexagonal composite tubes. Here, the area under crush load-displacement curve is considered as energy absorption E . The maximum crush load P_{max} is a single peak at the end of the initial linear part of the load curve. The mean crush load P_m has been determined with the use of Equation (1). The maximum crush displacement S_{max} is the total displacement of the impactor after contact with the crash box. The values of specific energy absorption SEA, which is the energy absorption per crush weight, and the crush load efficiency η , which is the ratio of the mean crush load and maximum crush load, are also presented in these tables.

Figure 3 shows the specimen (S-67) and (S-75) after crush, respectively. Relatively ductile crush mode can be recognized. The tubes are split at their corners. This splitting effect is initiated at the end of the linear elastic loading phase, when the applied load attains its peak value P_{max} . The splitting of the corners of the tube is followed by an immediate drop of the crush load, and propagation parallel to the tube axis results in splitting of the tube in several parts. Simultaneous of splitting, some of these parts are completely splayed into two fronds which spread outwards and inwards and some parts are split only partially. Subsequent to splitting, the external and internal fronds are bended and curled downwards and some additional transverse and longitudinal fracture happened.

Photographs from high speed camera for different impact moments are presented in Figures 4 and 5. Here it can be seen that local matrix and fiber rupture results in a formation of pulverized ingredients material just after initial contact between impactor and crash boxes. As compressive loading proceeds, further fragments are detached from the crash box. Furthermore, the crush performance of tests has been simulated with the use of LS-DYNA explicit code. Figure 6 shows the experimental and simulated crush load-displacement and energy absorption-displacement curves of tests (S-67) to (S-69).

The same results for hexagonal crash boxes, tests (S-75) to (S-77), are presented in Figure 7. The crush-load displacement curves indicate that the mean crush load of simulation is obviously lower than experimental results. The numerical simulation can not cover the experiments very good.

Test No.	V [m/s]	t [mm]	P _{max} [kN]	P _m [kN]	S _{max} [mm]	E [J]	SEA [J/kg]	η [%]
S-67	10.3	2.4	77.2	40.6	126.9	4956	41844	53
S-68	10.4	2.4	75.3	46.03	118.9	5053	45533	61
S-69	10.2	2.4	83.7	43.3	117.3	4923	44967	52
S-70	10.4	2.7	82.2	58.7	86.2	5075	55542	71
S-71	10.4	2.7	92.3	59.3	84.7	5024	55957	64

Table 1. Experimental dynamic test on square composite tube

Test No.	V [m/s]	t [mm]	P _{max} [kN]	P _m [kN]	S _{max} [mm]	E [J]	SEA [J/kg]	η [%]
S-72	7.3	2.0	51	42.6	72.8	3103	35681	83
S-73	7.3	2.0	55	45.5	68.3	3109	35750	83
S-74	7.3	2.0	46	37.9	78.2	2964	34083	82
S-75	8.4	2.4	72	53.7	76.95	4133	39604	75
S-76	8.4	2.4	81	69.4	61.03	4235	40582	86
S-77	8.9	2.4	72	65.6	71.4	4683	44875	91
S-78	8.3	2.7	83	66.9	59.96	4012	34173	81
S-79	8.3	2.7	80	68.4	58.6	4008	34139	86
S-80	8.8	2.7	84	58.8	75.5	4442	37836	70

Table 2. Experimental dynamic test on hexagonal composite tube



Fig. 3. Crush pattern of square tube S-67 (left) and hexagonal tube S-75 (right)

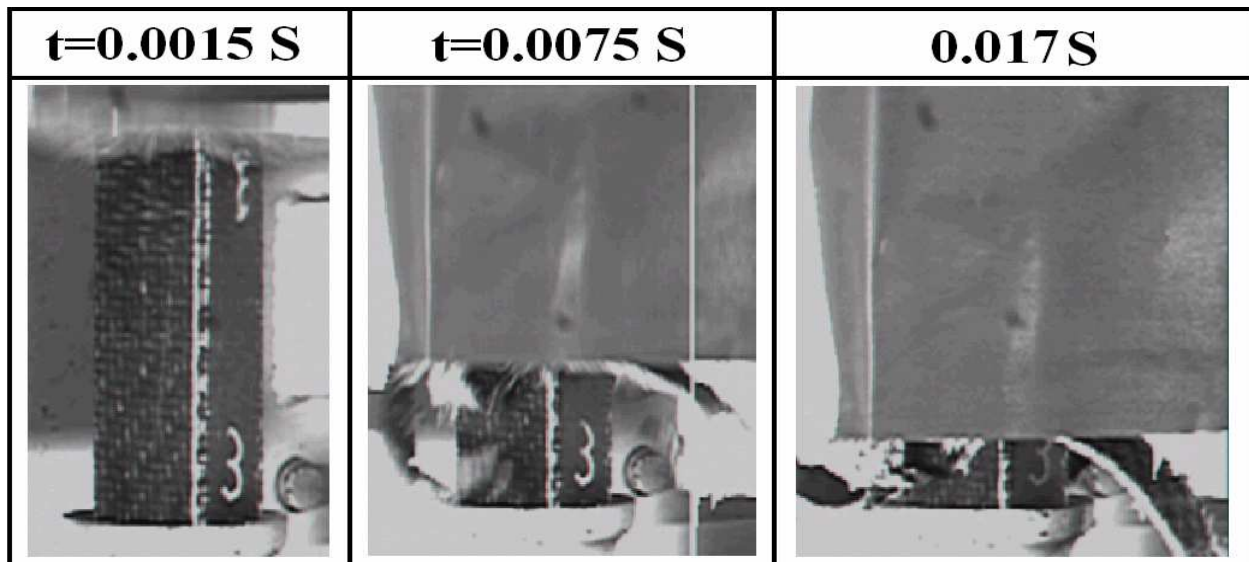


Fig. 4. Crush pattern of a square composite tube (S-67) for different crush moments

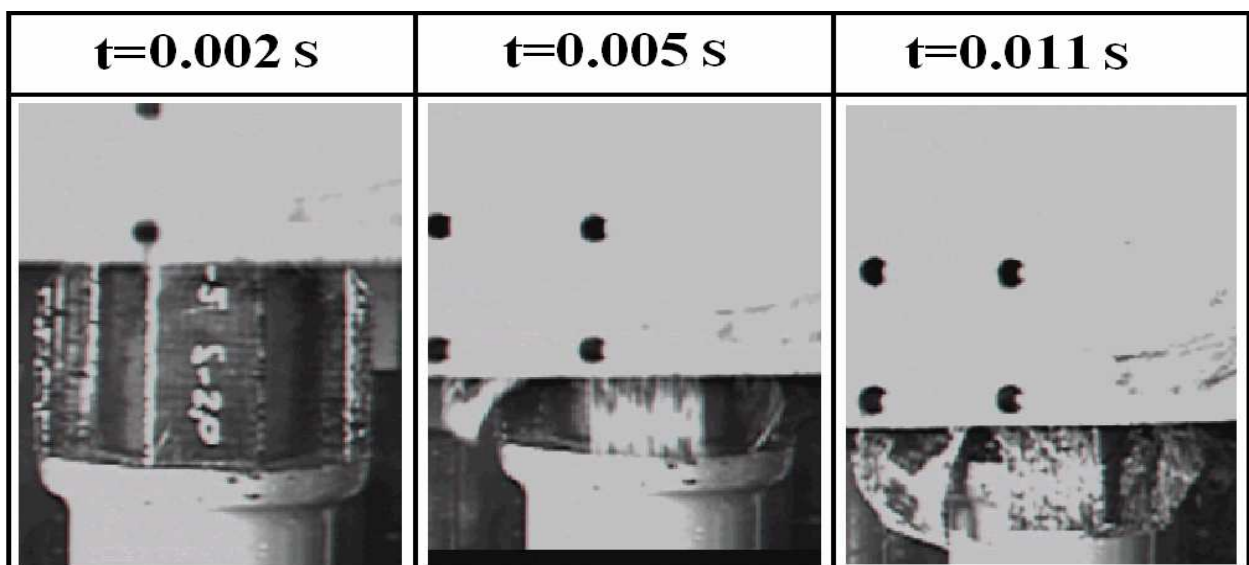


Fig. 5. Crush pattern of a hexagonal composite tube (S-75) for different crush moments

The energy absorption E and specific energy absorption SEA of the experiments and simulations at the same crush length (80 mm for square tubes and 60 mm for hexagonal ones) are presented in Table 3. Here, index S indicates simulation results. Again, it can be seen that the numerical simulations highly underestimate the tube crush behavior. The numerical crush patterns show the tube experiences the progressive crushing with some damages in tube walls instead of splitting and spreading, see Figure 8 and 9. It is evident that the total energy absorption of the composite tube is the sum of the energy needed for splitting of the tube corners, delamination and spreading of tube walls into two inwards and outwards fronds, bending and curling of each fronds, fracture and damage created in fronds during bending, fragmentations of tube walls and friction between the impactor and inwards and outwards fronds. The single layer finite element model does not have the capability to consider all aspects of crushing damages observed experimentally. Therefore, a new finite element model has to be developed to overcome this problem.

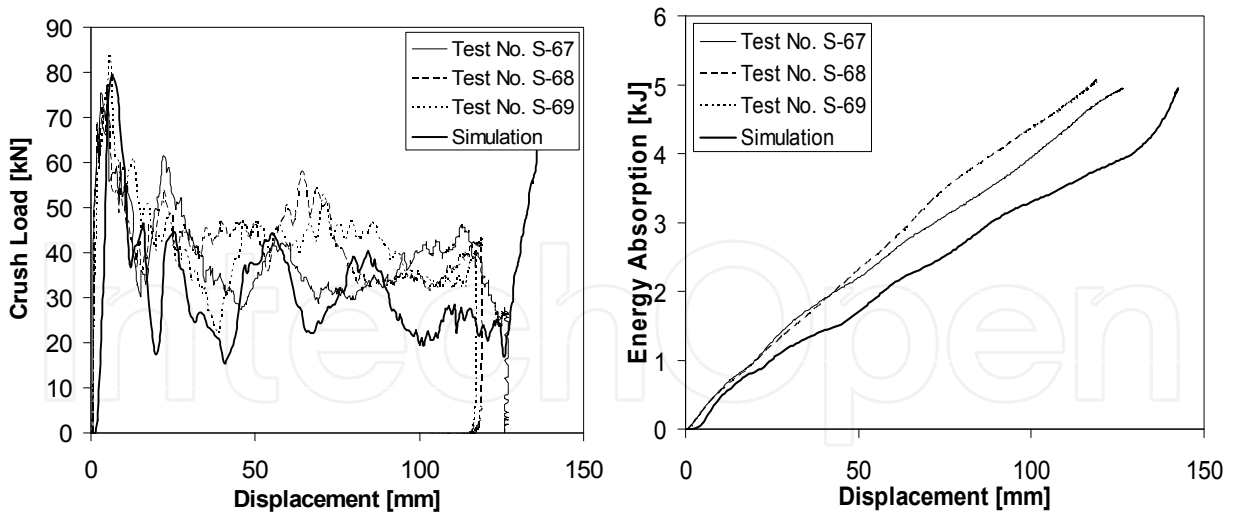


Fig. 6. Comparison between experimental and numerical (single layer method) crush load-displacement curves (left) and energy absorption-displacement curves (right) of square composite tubes

Test No.	E [J]	SEA [J/kg]	Es [J]	SEAS [J/kg]	Difference [%]
S-67	3259	43647	2686	35973	-17.6
S-68	3682	49313	-	-	-27.1
S-69	3520	47143	-	-	-23.7
S-75	3718	54035	2890	42002	-22.3
S-76	4170	60604	-	-	-30.7
S-77	3930	57116	-	-	-26.5

Table 3. Comparison between experimental and numerical (single layer method) energy absorption and specific energy absorption of the square and hexagonal tubes

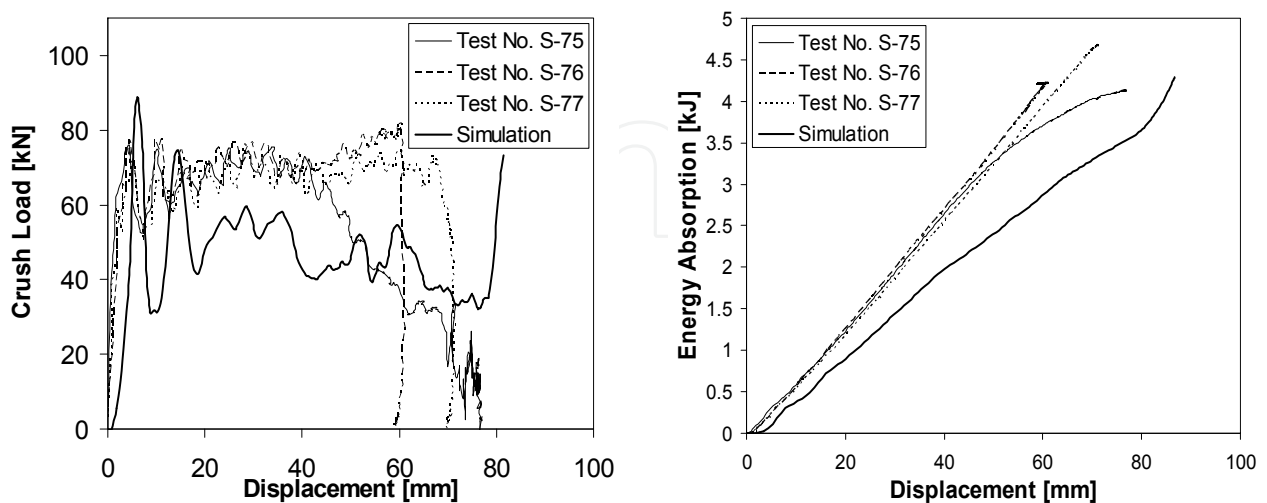


Fig. 7. Comparison between experimental and numerical (single layer method) crush load-displacement curves (left) and energy absorption-displacement curves (right) of hexagonal composite tubes

3. Advanced finite element model

The numerical crush behavior of the composite crash box are shown above for tube walls modeled with only one layer of shell elements, simulated crush pattern are quite different from experiment. The delamination, a main energy absorption source of composite crash boxes, can not be modeled and, therefore, the predicted energy absorption by the simulation is highly underestimated. Several methods have been used by the researchers to model the delamination growth in composite materials, including the virtual crack extension technique (Farley & Jones, 1992), stress intensity factor calculations (Hamada & Ramakrishna, 1997), stresses in a resin layer (Kindervater, 1995), and, the virtual crack closure technique (Fleming & Vizzini, 1996).

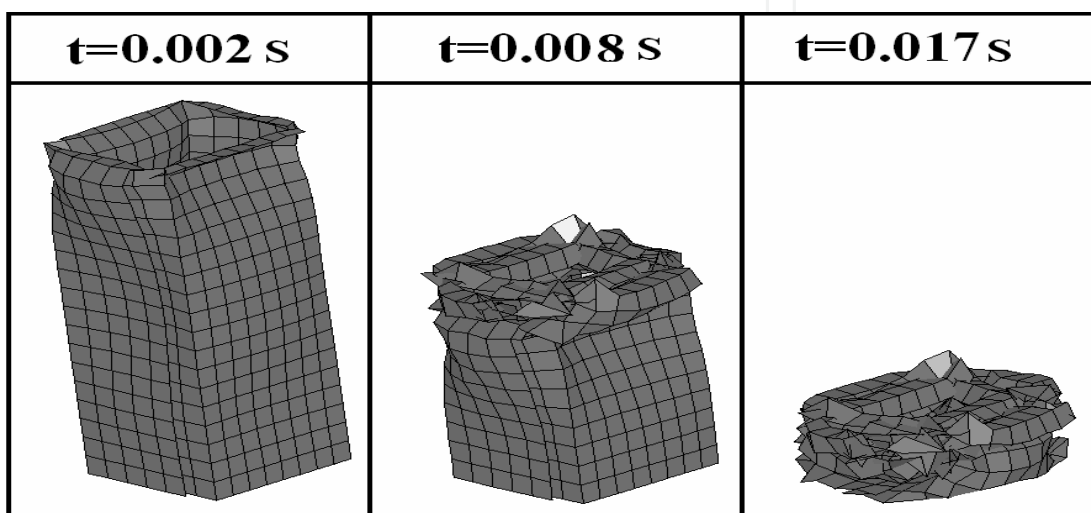


Fig. 8. Crush pattern of single layer finite element model of square composite tube

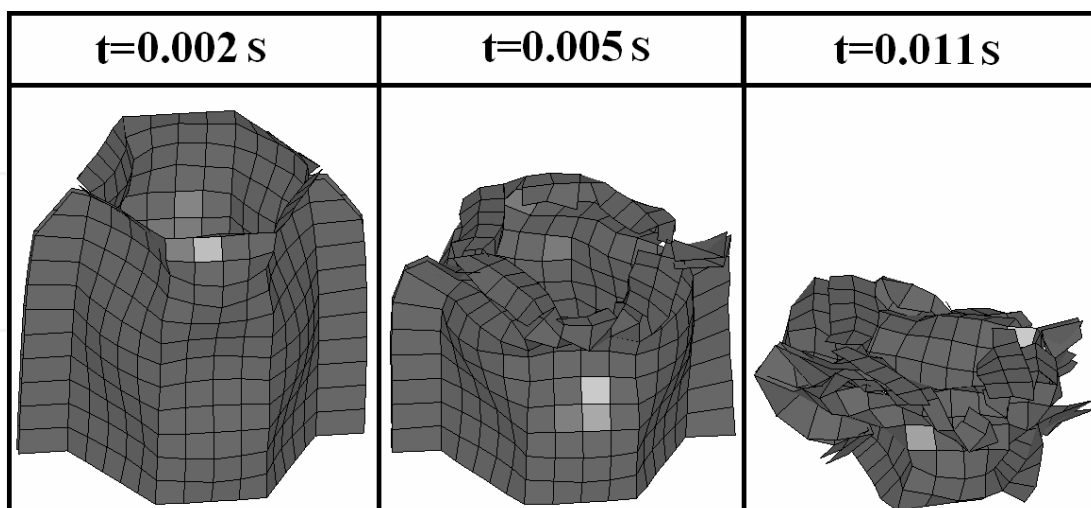


Fig. 9. Crush pattern of single layer finite element model of hexagonal composite tube

However, choices for modeling delamination using conventional finite element crush codes are more limited. Good correlations are obtained in many cases using models that do not fully capture all aspects of crushing damage observed experimentally. They only provide sufficient attention to the aspects of crushing that mostly influence the response. Models of

composite structures using in-plane damaging failure models to represent crushing behavior are used in (Haug et al., 1991), (Johnson et al., 1996 and 1997), (Feillard, 1999) and (Kohlgrueber & Kamoulakos, 1998). These models appear to be effective for structures whose failure modes are governed by large-scale laminate failure and local instability. However, crushing behavior in which wholesale destruction of the laminate contributes significantly to the overall energy absorption cannot be accurately modeled by this approach (Fleming, 2001). Further, if delamination or debonding forms a significant part of the behavior, specialized procedures must be introduced into the model to address this failure mechanism. Kohlgrueber and Kamoulakos (Kohlgrueber & Kamoulakos, 1998) and Kerth et al. (Kerth et al., 1996) used tied connections with a force-based failure method to model the delamination in composite materials. By this method, nodes on opposite sides of an interface where delamination is expected are tied together using any of a variety of methods including spring elements or rigid rods. If the forces produced by these elements exceed some criterion, the constraint is released. The primary disadvantage of this method is that there is no strong physical basis for determining the failure forces. Reedy et al. (Reedy et al., 1997) applied cohesive fracture model for the same reason. This method is similar to the previous method. However, instead of relying on simple spring properties the force-displacement response of the interfacial elements is based on classical cohesive failure behavior. Virtual crack closure technique is often used by researchers in the area of fracture mechanics. Energy release rates are calculated from nodal forces and displacements in the vicinity of a crack front. Although the method is sensitive to mesh refinement, but not so sensitive like the other fracture modelling techniques, those requiring accurate calculation of stresses in the singular region near a crack front. Further, the use of conventional force and displacement variables obviates the need for special element types that are not available in conventional crash codes.

In this study for the delamination, tube walls are modeled with two layers of shell elements. The thickness of each layer is equal to the half of the tube wall thickness [130]. To avoid tremendous increase of the required simulation time, a larger number of layers is avoided. The surface to surface tiebreak contact is used to model the bonding between the bundles of plies of the tube walls. In this contact algorithm the tiebreak is active for nodes which are initially in contact. Stress is limited by the perfectly plastic yield condition. For ties in tension, the yield condition is

$$[\sqrt{(\sigma_n^2 + 3|\sigma_s|^2)} / \varepsilon_p] \leq 1 \quad (6)$$

Where ε_p is the plastic yield stress and σ_n and σ_s are normal and shear stresses, respectively. For ties in compression, the yield condition is

$$[\sqrt{3|\sigma_s|^2} / \varepsilon_p] \leq 1 \quad (7)$$

The stress is also scaled by a damage function. The damage function is defined by a load curve with starts at unity for crack width of zero and decays in some way to zero at a given value of the crack opening (Hallquist, 1998)], see Figure 10. The surface to surface tied contact is implemented between the overlapped walls and single surface contact is used for each layer. The node to surface contact is applied between rigid impactor and composite layers. To model the rupture at the corners of the tube, the vertical sides of the tube have offset 0.5 mm and deformable spot-welds are used to connect the nodes of the vertical sides.

The spot-welds are defined by the use of material number #100 in LS-DYNA (MAT_SPOTWELD). Based on this material model, beam elements, based on Hughes-Liu beam formulation, are placed between the tube walls and contact-spotweld algorithm ties the beam elements to the tube shell elements. The normal strength of spot-welds is calculated from the transverse tensile strength of the composite material.

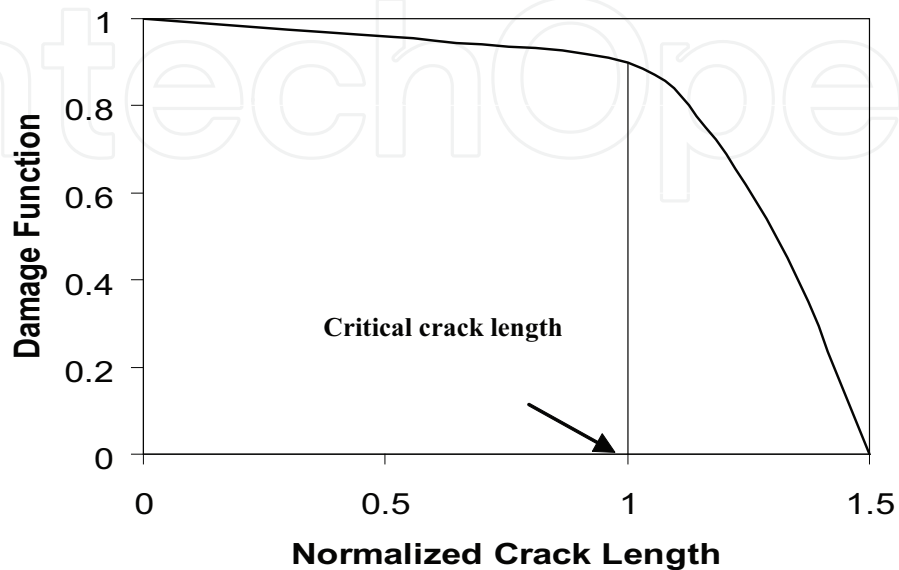


Fig. 10. Variation of damage function

To account for the reduced strength of the composite material at the corners, material strength is reduced by 50%. The shear strength is considered as half of the normal strength. In order to model the trigger, the length of the outer layer of the composite tube is a little bit smaller than the inner layer. The crush patterns of the multi layer square and hexagonal crash boxes are presented in Figures 11 and 12. Here it is possible to see the delamination which starts in some tube walls and propagates during the crush process.

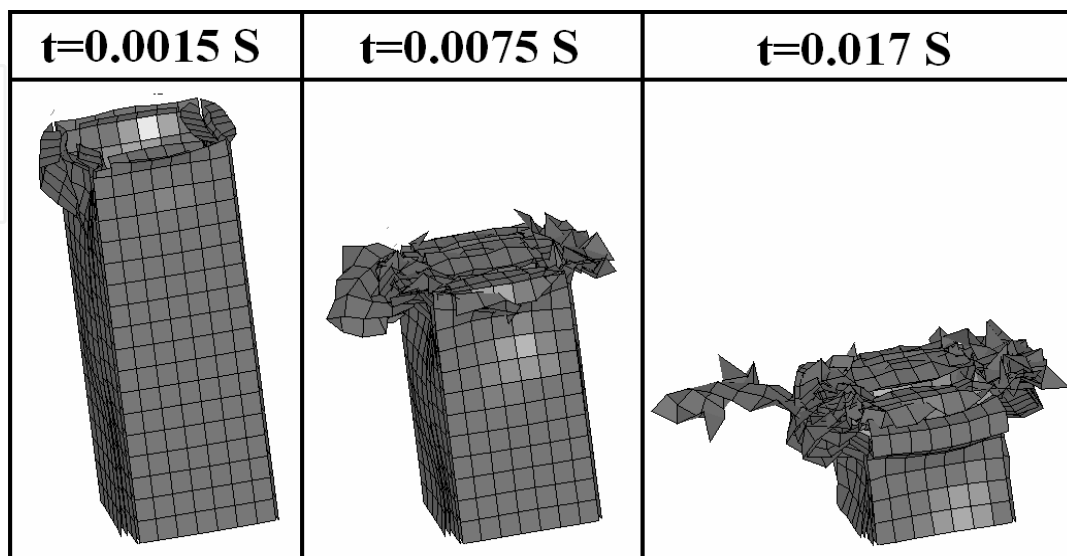


Fig. 11. Crush pattern of multi layer finite element model of square composite tube

The Figures 13 and 14 left compare the crush load-displacement curves of experimental and numerical impact on square and hexagonal crash boxes, respectively. Acceptable correlations are reached between experiments and simulations. In addition the experimental and numerical energy absorption is presented in Figure 13 and Figure 14 right. The multi layers method can predict the energy absorption of the crash box very well.

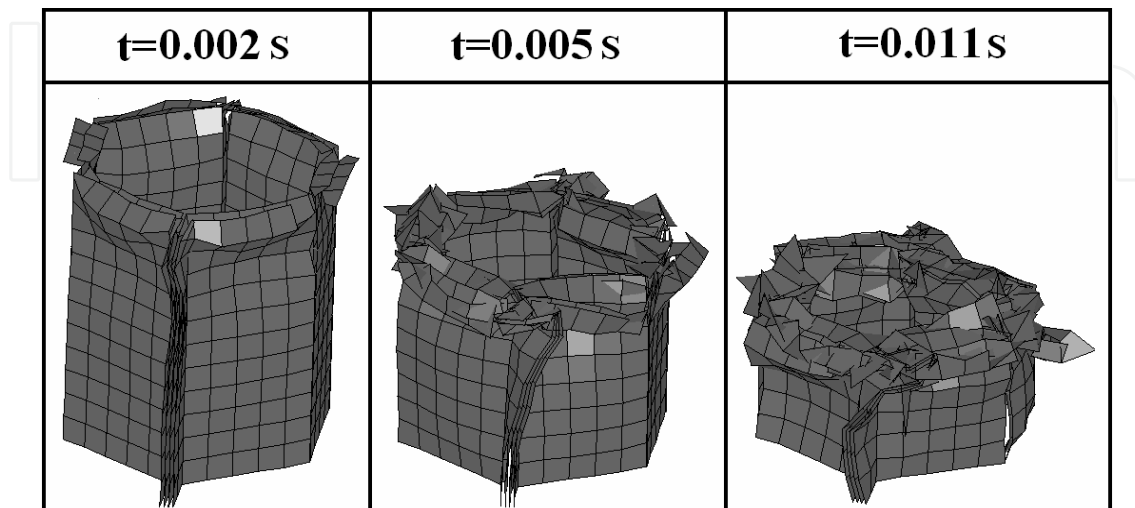


Fig. 12. Crush pattern of multi layer finite element model of hexagonal composite tube

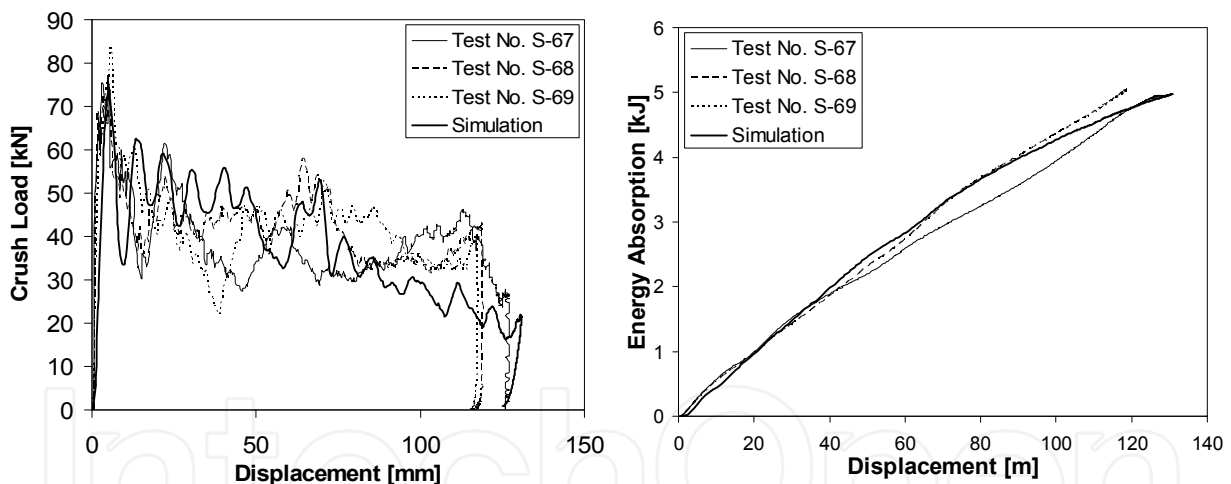


Fig. 13. Comparison between experimental and numerical (multi layers method) crush load-displacement curves (left) and energy absorption-displacement curves (right) of square composite tubes

4. Multi design optimization of crush behavior of square composite crash box

There are high interests to find the effect of composite tube geometry on its energy absorption capability. Generally, variation in tube geometry influences the fracture mechanisms and, therefore, the energy absorption capability. Thornton and Edwards (Thornton and Edwards, 1982) investigated the crush performance of square, rectangular and circular composite tubes. They concluded that for a given fiber lay up and tube geometry, circular tubes have the highest specific energy absorption followed by square and

rectangular tubes. Farley (Farley, 1986) investigated the effect of geometry on the energy absorption capability of the composite tubes. He conducted a series of quasi-static crash tests of Graphite/Epoxy and Kevlar/Epoxy composite tubes with the ply orientation of ± 45 degree. He found that the tube diameter to wall thickness ratio d/t has significant effects on the energy absorption capability. The energy absorption was found to be a decreasing nonlinear function of tube d/t ratio. A reduction in d/t ratio increases the specific energy absorption of the tube. Similar result has been reported by Farley and Jones (Farley & Jones, 1992) for elliptical composite tubes.

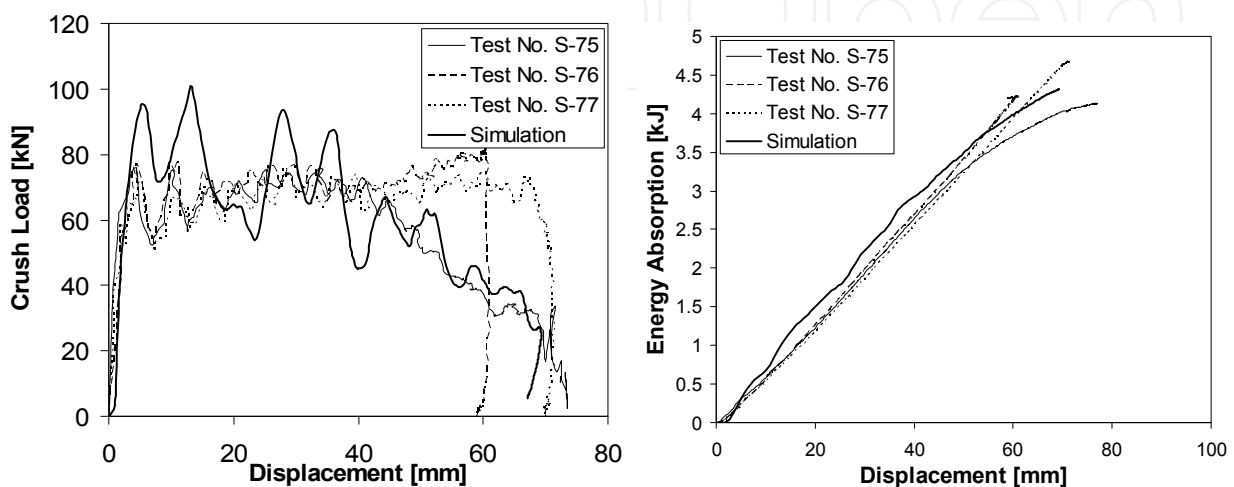


Fig. 14. Comparison between experimental and numerical (multi layers method) crush load-displacement curves (left) and energy absorption-displacement curves (right) of hexagonal composite tubes

Zarei and Kroeger (Zarei & Kroeger, 2006) used Multi design objective MDO crashworthiness optimization method to optimize circular aluminum tubes. Here, the same optimization procedure is used to find optimum composite crash box. The finite element method is used to calculate the absorbed energy and specific absorbed energy of the tubes. The design variables are the tube thickness (number of layers), width and length of the composite tubes. The composite tubes with the thickness between 1 mm and 4 mm are selected while the tube width is varied between 70 mm and 120 mm and the tube length between 100 mm and 350 mm. Here 0.5 mm thickness is considered for each layer of composite tube. To have acceptable crush performance in oblique crash conditions, the tube width lower than 70 mm is not considered. An impact force constraint is usually required to reduce the occupant injury when passenger vehicles are considered. Therefore, in the optimization process, the mean crush load P_m should not exceed the allowable limit P_{ma} i.e.:

$$g = P_m / P_{ma} - 1 \leq 0. \quad (8)$$

Where $P_{ma} = 68.5$ kN is selected in this research. The optimization problem can be rewritten as follows

Maximize energy absorption E and specific energy absorption SEA of tube
Subjected to

$$\begin{aligned} 0.5 \text{ mm} &\leq t \leq 3.0 \text{ mm}, \\ 100 \text{ mm} &\leq l \leq 350 \text{ mm}, \\ 50 \text{ mm} &\leq d \leq 120 \text{ mm}, \\ P_m &\leq 68.5 \text{ kN}. \end{aligned}$$

The optimization procedure which is presented in Figure 15 is applied to the maximization of absorbed energy and specific absorbed energy of the composite tube under axial impact load. Since the interest is to find the crush behavior of tubes up to the final effective crush length, all tubes are encountered with a large amount of impact energy. Here 75 percent of tube length is considered as effective crush length. In order to reduce the optimization time, the single layer finite element models are used to find the energy absorption of composite tubes in every subproblem and the final optimum tube is modeled as a multi layer composite tube.

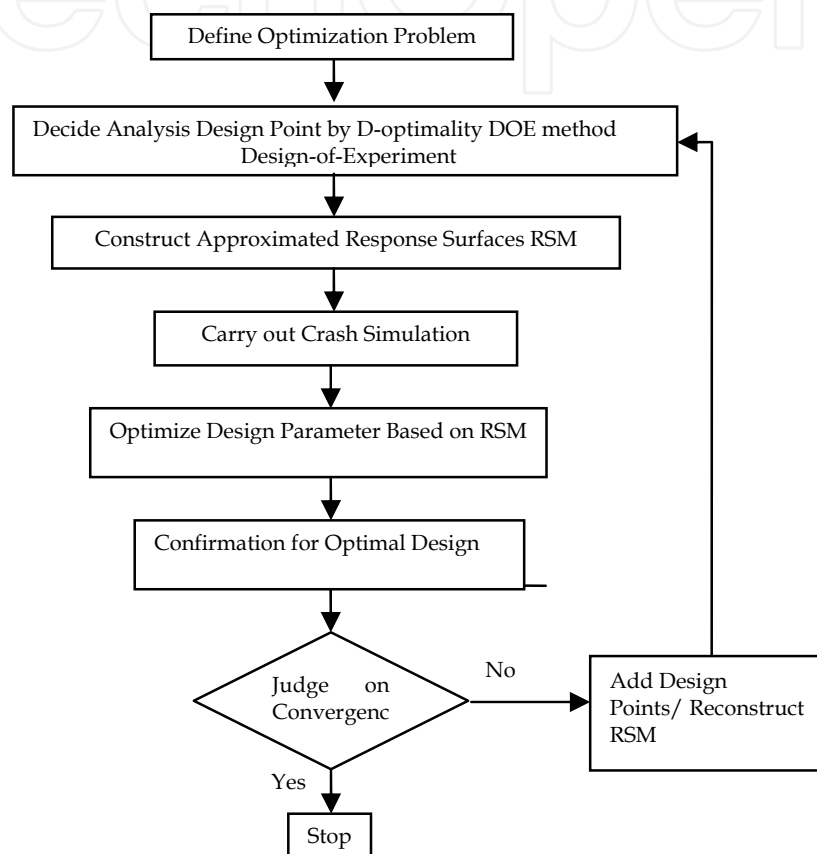


Fig. 15. Flowchart of the optimization process

Table 4 shows the final optimum composite tube that absorbs maximum energy with minimum weight. Here it can be seen that the optimum tube thickness t is 3 mm ($N_1=6$ layers). The thicker tube will have mean crush load higher than allowable limit. The variable d coincides with the lower bound which shows an increase of the crashworthiness efficiency by reduction of tube width. But here values lower than 70 mm are not allowed to guarantee enough bending resistance of the composite crash box in oblique crash conditions. The tube length coincides with the upper bound but in order to avoid global buckling, longer tubes are not considered. Previously the MDO procedure was used to find optimum aluminum tubes. There, to avoid global buckling in the aluminum tubes the maximum allowed tube length to width ratio is set to $l/d \leq 3$ based on experimental observations (Mamalis et al., 2005) and (Hanssen et al., 1999 and 2000). In order to compare crashworthiness behavior of the optimum composite and aluminum crash boxes, this new optimization constraint is considered for composite crash tube. Table 5 shows the results of optimum composite and

aluminum crash boxes. It can be seen that the composite tube absorbs about 17 percent more energy than aluminum crash box while it has about 27 percent lower weight.

Tube type	T; N ₁ [mm; -]	d [mm]	l [mm]	E [J]	SEA [J/kg]
Square composite	3; 6	70	350	15316	35580

Table 4. Optimum square composite tube

Tube Type	t [mm]	d [mm]	l [mm]	E [J]	Increase [%]	SEA [J/kg]	Increase [%]
Square aluminum	2.1	70	210	7602	-	26124	-
Square composite	3	70	210	9198	17.4	35716	26.9

Table 5. Comparison between optimum composite and optimum aluminum crash boxes

5. Crush performance investigation of foam-filled composite crash box

Here, Alporas aluminum foam with a relative density of 0.085 is used to produce foam filled square composite crash box. Dynamic compression tests were conducted on them. The composite square tubes with the dimensions which previously presented in Figure 1 are used. The nominal wall thickness of the composite tubes is 2.4 mm. Dynamic tests were done in drop weight test rig. Simply support boundary conditions were applied for the tubes. Table 6 shows the results of experimental tests. The crush pattern of test number (F-37) is shown in the Figure 16. Here, similar to empty composite tubes, the tube is split from its corners. In comparison to the empty composite tubes, lower delamination area can be seen. The tube is ruptured from its corners and the foam filler is crushed progressively. Numerical simulations of crash tests are performed using the explicit finite element code LS-DYNA. The new developed finite element model in this study is used to describe the composite square tubes, see section 4. The foam filler is modeled with solid elements and rigid body elements are used to model the rigid impactor. The contact between the rigid body and the specimen is modeled using a node to surface algorithm with a friction coefficient of $\mu=0.2$. To account for self contact between the tube walls during deformation, a single surface contact algorithm is used. The node to surface contact is implemented between tube walls and foam filler. The composite walls are modeled with the use of material model #54 in LS-DYNA. The aluminum foam was modeled with the foam model of Dehspande and Fleck (2000) [19] material number #154 in LS-DYNA. Figure 17 shows that the predicted energy absorption by the simulation is in good agreement with the experimental one.

Table 7 shows a comparison between energy absorption E and specific energy absorption SEA of the empty and foam-filled composite square tubes at the 80 mm crash length. Here, it can be seen that the foam insertion of the composite tube results in higher energy absorption but unlike the aluminum foam-filled tubes, the specific energy absorption in the composite filled tubes is decreased in comparison with empty one. As mentioned in the chapter four, the benefit of using foam inside the crash absorbers is the interaction between foam and crash absorber walls during crush process. But as one can see in the Figure 16, in the foam-filled composite tubes, the composite tube is split into four parts and the tube and foam crushed independently. Here no interaction between tube and foam is taken place. From

Figure 3 it can be seen that the empty composite tubes are split into several parts and each part is splayed into two fronds which spread outwards and inwards. From Figure 16 it is clear that the foam filler forced the tube parts outward during the crush process and prevent from splaying of the parts. Therefore no frond is created and delamination between the composite layers, which is one of the main energy absorption sources of the composite, is not taken placed. Therefore, the specific energy absorption of the filled composite tube is lower than empty tubes.

Another interesting result which is extracted from experimental results of dynamic tests on simple foam filler is that the energy absorption of foam filler is about 4950 J at 80 mm crash length. That means the some of the energy absorption of the empty composite tube alone and foam filler alone is higher than energy absorption of the foam-filled composite tube. In other word not only inserted foam plays no positive roll in the crush process of the filled composite crash box but also it has destructive effect.

Test No.	V [m/s]	t [mm]	P_{max} [kN]	P_m [kN]	S_{max} [mm]	E [J]	SEA [J/kg]	η [%]
F-37	10.4	2.4	85.1	46.9	105.4	4994	34006	55.1
F-38	10.3	2.4	95.1	47.3	97.7	4890	35922	49.7
F-39	10.3	2.4	87.8	46.2	108.5	4954	32770	42.6

Table 6. Experimental dynamic test on foam filed square composite tube



Fig. 16. Crush pattern of foam-filled composite crash box

Test No.	Filler type	E [J]	Increase [%]	SEA [J/kg]	Increase [%]
Average of S-67, S-68, S-69	-	3487	-	46701	-
Average of F-37, F-38-F-39	Foam	3832	9.0	34233	-26.7

Table 7. Comparison between empty and foam-filled composite tubes

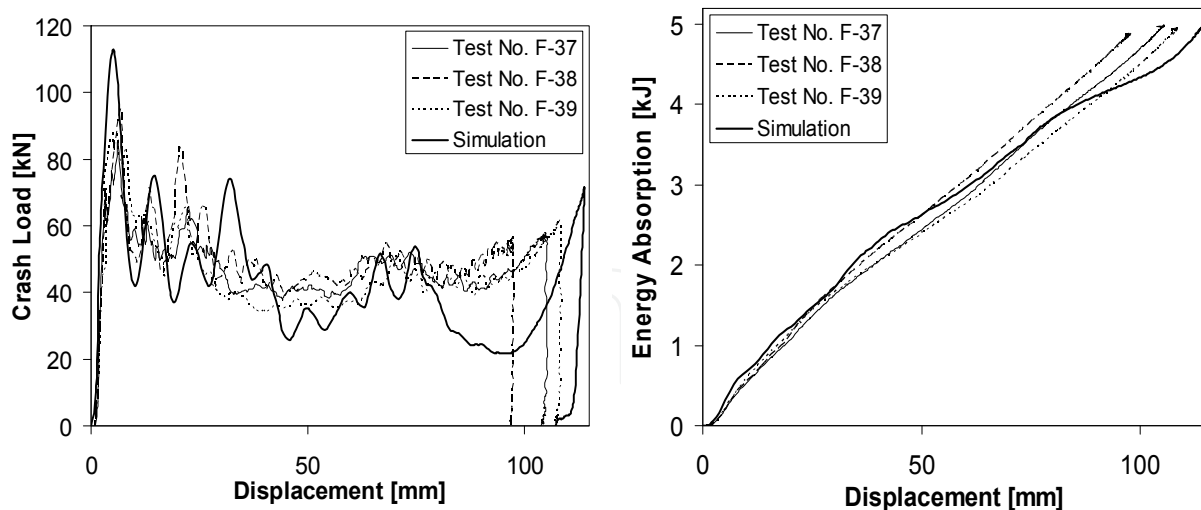


Fig. 17. Comparison between experimental and numerical (multi layers method) crush load-displacement curves (left) and energy absorption-displacement curves (right) of square composite foam-filled tubes

6. Conclusion

Experimental crash tests on square and hexagonal composite crash boxes showed that unlike metallic crash boxes which are crushed in a progressive buckling manner, the composite tubes are crushed in a progressive damaging manner.

A new multi layer finite element model was developed to simulate the crush process of the composite crash box.

The MDO procedure was used to find an optimum design of the composite crash box. The comparison between crashworthiness behavior of the optimum composite and aluminum crash boxes showed that the composite crash box absorbs about 17 percent more energy than the aluminum crash box while it has about 27 percent higher SEA.

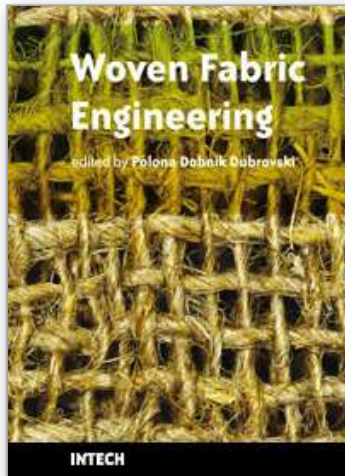
For light weight crash box or bumper beam designs, low density metal fillers, such as aluminum honeycomb or foam, are superior to tubes and beams with thicker walls in terms of achieving the same energy absorption. The crush performance of foam-filled square composite crash box was investigated experimentally and numerically. The results showed that the foam insertion results in higher energy absorption but unlike the aluminium foam-filled tubes, the specific energy absorption of the composite filled tubes is decreased in comparison with empty one.

7. References

- Bisagni, C.; Pietro, GD.; Frascini, L. & Terletti, D. (2005). Progressive crushing of fiber-reinforced composite structural component of a formula one racing car. *Compos. Struct.*, Vol. 68, 491–503
- Chang, FK. & Chang, KY. (1987). Post-failure analysis of bolted composite joints in tension and shear-out mode failure. *J. Compos. Mater.*, Vol. 21, 809–33

- El-Hagel, H.; Mallick, PK. & Zamani, N. (2004). Numerical modeling of quasistatic axial crash of square aluminum-composite hybrid tubes. *Int. J. Crashworthiness*, Vol. 9, No. 6, 653-64
- Farley, G.L. (1991). The effects of crushing speed on the energy-absorption capability of composite tubes. *J. Compos. Mater.*, Vol. 25, No. 10, 1314-29.
- Farley, G.L. (1983). Energy absorption of composite materials. *J. Compos. Mater.*, Vol. 17, No. 3, 267-79
- Farley, GL. (1986). Effect of specimen geometry on the energy absorption capability of composite tubes. *J. Compos. Mater.*, Vol. 20, 390-400
- Farley, GL. & Jones, RM. (1992). Prediction of the energy-absorption capability of composite tubes. *J. Compos. Mater.*, Vol. 26, No. 3, 388-404
- Fleming, DC. & Vizzini, AJ. (1996). Off-axis energy absorption characteristics of composites for crashworthy rotorcraft design. *J. American Helicopter Soc.*, Vol. 41, No. 3, 239-46
- Fleming, DC. (2001). Delamination modeling of composite for improved crash analysis. *J. Compos. Mater.*, Vol. 35, No. 19, 1777-92
- Feillard, P. (1999). Crash modeling of automotive structural parts made of composite materials, *Proceedings of the SAE international congress and exposition*, March 1-4, Detroit, MI
- Jacob, GC.; Simunovic, JFS. & Starbruk, JM. (2002). Energy absorption in polymer composite for automotive crashworthiness. *J. Compos. Mater.*, Vol. 36, No.7, 813-50
- Johnson, AF.; Kindervater, CM.; Kohlgrueber, D. & Luetzenburger, M. (1996). Predictive methodologies for the crashworthiness of aircraft structures, *Proceedings of the 52nd american helicopter society annual forum*, pp. 1340-52, June 4-6, Washington DC
- Johnson, AF. & Kohlgrueber, D. (1997). Modeling the crash response of composite structures. *J. Phys. IV France, Colloque C3, Supplément au Journal de Physique III*, Vol. 7, C3-981-6 (in English).
- Hallquist, JO. (1998). *LS-DYNA theoretical manual*. Livermore Software Technology Corporation
- Hamada, H.; Ramakrishna, SA. (1997). FEM method for prediction of energy absorption capability of crashworthy polymer composite materials. *J. Reinf. Plast. Compos.*, Vol. 16, No. 3, 226-42
- Hanssen, AG.; Langseth, M. & Hopperstad, OS. (1999). Static crushing of square aluminum extrusions with aluminum foam filler. *Int. J. Mech. Engng.*, Vol. 41, 967-993
- Hashin, Z. (1980). Failure criteria for unidirectional fiber composites. *J. Appl. Mech.*, Vol. 47, 329-34
- Haug, E.; Fort, O.; Tramecon, A.; Watanabe, M. & Nakada, I. (1991). Numerical crashworthiness simulation of automotive structures and components made of continuous fiber reinforced composite and sandwich assemblies. *SAE technical paper series 910152*
- Hoermann, M. & Wacker, M, (2005). Simulation of the crash performance of crash boxes based on advanced thermoplastic composite, *Proceedings of the 5th European LS-DYNA users conference*, pp. 25-6, UK, May, Birmingham
- Hull, D. (1982). Energy absorption of composite materials under crash displacement variables obviates the need for special element types that are not available in crash

- codes, *Proceeding of the 4th international conference on composite materials: progress in science and engineering of composites*, pp. 861–87, Japan, Tokyo
- Kerth, S.; Dehn, A.; Ostgathe, M. & Maier M. (1996) Experimental investigation and numerical simulation of the crush behavior of composite structural parts, *Proceedings of the 41st international SAMPE symposium and exhibition*, pp. 1397–408
- Kindervater, CM. (1995). Crash resistant composite helicopter structural concepts thermoset and thermoplastic corrugated web designs, *Proceedings of the AHS national technical specialists meeting on advanced rotorcraft structures*, Williamsburg, VA
- Kohlgrueber, D. & Kamoulakos, A. (1998). Validation of numerical simulation of composite helicopter sub-floor structures under crash loading, *Proceedings of the 54th American helicopter society annual forum*, May 20–22 Washington DC
- Mamalis, AG.; Manolakos, DE.; Demosthenous, GA. & Ioannidis, MB. (1997). The static and dynamic axial crumbling of thin-walled fiberglass composite square tubes. *Composites Part B*, Vol.28B, No. 4, 439–51
- Mamalis, AG.; Manolakos, DE.; Ioannidis, MB. & Papapostolou, DP. (2005). On the response of thin-walled composite tubular components subjected to static and dynamic axial compressive loading: experimental. *Compos. Struct.*, Vol. 69, 407–20
- Mamalis, AG.; Manolakos, DE.; Ioannidis, MB. & Papapostolou, DP. (2006). The static and dynamic axial collapse of CFRP square tubes: finite element modeling. *Compos. Struct.*, Vol. 74, 2213–50
- Mallick, PK. (1990) *Fiber reinforced composites*. 2nd ed. NY, Marcel Dekker
- Ramakrishna, S. (1997). Microstructural design of composite materials for crashworthy applications. *Mater. Des.*, Vol.18, 167–73
- Reedy, ED.; Mello FJ. & Guess, TR. (1997). Modeling the initiation and growth of delaminations in composite structures. *J. Compos. Mater.*, Vol. 31, No. 8, 812–31
- Shin, K.C.; Lee, JJ.; Kim, KH.; Song, MC. & Huh, JS. (2002). Axial crash and bending collapse of an aluminum/GFRP hybrid square tube and its energy absorption capability. *Compos. Struct.*, Vol. 57, 279–87
- Thornton, PH. & Edwards, PJ. (1982). Energy absorption in composite tubes. *J. Compos. Mater.*, Vol. 16, 21–45
- Yamazaki, K. & Han, J. (1998). Maximization of the crushing energy absorption of tubes. *Struct. Optim.*, Vol. 16, 37–49
- Zarei, HR. & Kroeger, M. (2006). Multiobjective crashworthiness optimization of circular aluminum tubes. *Thin-Walled Struct. J.*, Vol. 44, 301–8
- Zarei, HR.; Kröger, M. & Albertsen, H. (2007). Crashworthiness investigation of the composite thermoplastic crash box, *Proceeding of the Sixth Canadian-International Composites Conference*, pp. 1-14, August, Winnipeg
- Zarei, HR.; Kröger, M. & Albertsen, H. (2008). An experimental and numerical crashworthiness investigation of the thermoplastic composite crash boxes. *Comp. struc. J.*, Vol. 85, 245-258



Woven Fabric Engineering

Edited by Polona Dobnik Dubrovski

ISBN 978-953-307-194-7

Hard cover, 414 pages

Publisher Sciyo

Published online 18, August, 2010

Published in print edition August, 2010

The main goal in preparing this book was to publish contemporary concepts, new discoveries and innovative ideas in the field of woven fabric engineering, predominantly for the technical applications, as well as in the field of production engineering and to stress some problems connected with the use of woven fabrics in composites. The advantage of the book *Woven Fabric Engineering* is its open access fully searchable by anyone anywhere, and in this way it provides the forum for dissemination and exchange of the latest scientific information on theoretical as well as applied areas of knowledge in the field of woven fabric engineering. It is strongly recommended for all those who are connected with woven fabrics, for industrial engineers, researchers and graduate students.

How to reference

In order to correctly reference this scholarly work, feel free to copy and paste the following:

Hamidreza Zarei and Matthias Kroeger (2010). Crashworthiness Investigation and Optimization of Empty and Foam Filled Composite Crash Box, *Woven Fabric Engineering*, Polona Dobnik Dubrovski (Ed.), ISBN: 978-953-307-194-7, InTech, Available from: <http://www.intechopen.com/books/woven-fabric-engineering/crashworthiness-investigation-and-optimization-of-empty-and-foam-filled-composite-crash-box>

INTECH
open science | open minds

InTech Europe

University Campus STeP Ri
Slavka Krautzeka 83/A
51000 Rijeka, Croatia
Phone: +385 (51) 770 447
Fax: +385 (51) 686 166
www.intechopen.com

InTech China

Unit 405, Office Block, Hotel Equatorial Shanghai
No.65, Yan An Road (West), Shanghai, 200040, China
中国上海市延安西路65号上海国际贵都大饭店办公楼405单元
Phone: +86-21-62489820
Fax: +86-21-62489821

© 2010 The Author(s). Licensee IntechOpen. This chapter is distributed under the terms of the [Creative Commons Attribution-NonCommercial-ShareAlike-3.0 License](#), which permits use, distribution and reproduction for non-commercial purposes, provided the original is properly cited and derivative works building on this content are distributed under the same license.

IntechOpen

IntechOpen